Inclusive charmonium production via double $c\bar{c}$ in e^+e^- annihilation

Kui-Yong Liu
Department of Physics, Peking University, Beijing 100871, People's Republic of China
and Department of Physics, Liaoning University, Shenyang 110036, People's Republic of China

Zhi-Guo He
Department of Physics, Peking University, Beijing 100871, People's Republic of China

Kuang-Ta Chao
China Center of Advanced Science and Technology (World Laboratory), Beijing 100080, People's Republic of China
and Department of Physics, Peking University, Beijing 100871, People's Republic of China
(Received 29 January 2004; published 28 May 2004)

Motivated by the recent observation of double-charm quark pair production by the Belle Collaboration, we calculate the complete $O(\alpha_s^2)$ inclusive production cross sections for η_c, J/ψ, and χ_{cJ} $(J=0,1,2)$ plus $c\bar{c}$ in e^+e^- annihilation through a virtual photon. We consider both color-singlet and color-octet contributions, and give the analytical expressions for these cross sections. The complete color-singlet calculations are compared with the approximate fragmentation calculations as functions of the center-of-mass energy $\sqrt{s}$. We find that most of the fragmentation results substantially overestimate the cross sections (e.g., by a factor of ~ 4 for χ_{c1} and χ_{c2}) at the Belle and BaBar energy $\sqrt{s}=10.6$ GeV. The fragmentation results become a good approximation only when $\sqrt{s}$ is higher than about 100 GeV. We further calculate the color-octet contributions to these cross sections with analytical expressions. We find that while the color-octet contribution to J/ψ inclusive production via double charm is negligible (only about 7%), the color-octet contributions to χ_{c1} and χ_{c2} can be very significant.

DOI: 10.1103/PhysRevD.69.094027 PACS number(s): 13.85.Ni, 12.40.Nn, 13.87.Fh, 14.40.Gx

I. INTRODUCTION

Charmonium is one of the simplest quark-antiquark composite particles. Charmonium physics has played an important role in the study of quantum chromodynamics (QCD) both perturbatively and nonperturbatively, since the first charmonium state J/ψ was discovered in 1974. During the past decade, the study of charmonium has become more interesting because of the large difference between the predictions of the color-singlet model and the observations of J/ψ and ψ' production at several experimental facilities—e.g., at the Fermilab Tevatron [1].

The newly developed nonrelativistic QCD (NRQCD) factorization formalism [2] allows the infrared safe calculation of inclusive heavy quarkonium production and decay rates. In the NRQCD production mechanism, a heavy quark-antiquark pair can be produced at short distances in a conventional color-singlet or a color-octet state, and then evolves into an observed quarkonium nonperturbatively. With this color-octet mechanism, one may explain the Tevatron data on the surplus production of J/ψ and ψ' at large p_T, though puzzles about their polarizations still remain (for a recent review see [3] and references therein).

To further test the color-octet mechanism, it is interesting to study the charmonium production in e^+e^- annihilation. The J/ψ inclusive production in e^+e^- annihilation has been investigated within the color-singlet model [4–6] and the color-octet model [7–9]. The angular distribution and energy distribution of color-singlet J/ψ production at $\sqrt{s}=10.6$ GeV have been discussed in [6]. In [7] it is found that a clean signature of the color-octet mechanism may be observed in the angular distribution of J/ψ production near the end point region. In [8] contributions of various color-octet as well as color-singlet channels to the J/ψ production cross sections are calculated in a wide range of e^+e^- collider energies. Moreover, the J/ψ polarizations are predicted in [9]. Recently, BaBar [11] and Belle [12] have measured the direct J/ψ production in continuum e^+e^- annihilations at $\sqrt{s}=10.6$ GeV. The total cross section and the angular distribution seem to favor the NRQCD calculation over the color-singlet model [11], but some issues (e.g., about the momentum distribution and polarization of J/ψ) still remain.

The situation has become even more complicated due to the very recent observation for the double-$c\bar{c}$ production associated with J/ψ by Belle [13]. The measured exclusive cross section for the $e^+ + e^- \to J/\psi + \eta_c$ process is an order of magnitude larger than the theoretical value [14], and the measured inclusive cross section for $e^+ + e^- \to J/\psi + c\bar{c}$ (~ 0.9 pb) [12,13] is more than 5 times larger than NRQCD predictions which are only about 0.1–0.2 pb [6,8–10], taking into account the differences in the values of the input parameters or methods. Among other attempts to solve the $J/\psi c\bar{c}$ inclusive production problem [15,16], e^+e^- annihilation into two photons was also studied [17,18], but the two-photon contribution turned out to be negligible at $\sqrt{s}=10.6$ GeV, though it could prevail over the one-photon contribution at higher energies (say, $\sqrt{s}>20$ GeV) [17].

The double-$c\bar{c}$ production associated with J/ψ (both ex-

clusively and inclusively) is very puzzling and needs a better understanding for both perturbative and nonperturbative QCD. On the other hand, experimentally, it is not clear whether the copious (even dominant) double-$c\bar{c}$ production will also happen for charmonium states other than J/ψ, such as η_c and χ_{cJ} $(J=0,1,2)$. Among them the χ_{c1} and χ_{c2} are more interesting since they have large branching fractions decaying into $J/\psi+\gamma$ and might be easier to detect. In fact, in Ref. [12] the inclusive production for χ_{c1} and χ_{c2} was searched for with the available integrated luminosity of about 30 fb^{-1} at Belle. As more data are collected in the near future at B factories we hope that more accurate measurements for the P-wave and other S-wave charmonium states will be possible. These measurements will be helpful to clarify the problems associated with J/ψ double-$c\bar{c}$ production.

On the theoretical side, calculations for inclusive S-wave and P-wave charmonia production via double $c\bar{c}$ are necessary in the framework of NRQCD, including both the color-singlet and color-octet contributions. When we know the differences between NRQCD predictions and experimental data, we will have to further consider other mechanisms and methods in QCD to explain the differences.

This paper is organized as follows. In Sec. II, we will calculate the complete $O(\alpha_s^2)$ color-singlet inclusive production cross sections for η_c and χ_{cJ} $(J=0,1,2)$ (along with J/ψ) via double $c\bar{c}$ in e^+e^- annihilation through a virtual photon. Then we will compare the complete calculation with the calculation obtained in the charm quark fragmentation limit, give their ratio as functions of the center-of-mass energies, and determine the energy scales at which fragmentation approximations become reliable. In Sec. III, we will further estimate the color-octet contributions to J/ψ and χ_{cJ} inclusive cross sections via double charm. Finally, we summarize our results in Sec. IV.

II. COLOR-SINGLET CONTRIBUTION TO CHARMONIUM PRODUCTION VIA DOUBLE $c\bar{c}$ IN e^+e^- ANNIHILATION

The quarkonium can be described in terms of a Fock states superposition within the NRQCD framework as follows:

$$|\psi_Q\rangle = O(1)|Q\bar{Q}[^3S_1^{(1)}]\rangle + O(v)|Q\bar{Q}[^3P_J^{(8)}]g\rangle + O(v^2)|Q\bar{Q}[^1S_0^{(8)}]g\rangle + O(v^2)|Q\bar{Q}[^3S_1^{(1,8)}]gg\rangle + \cdots, \tag{1}$$

$$|\chi_{cJ}\rangle = O(1)|Q\bar{Q}[^3P_J^{(1)}]\rangle + O(v)|Q\bar{Q}[^3S_1^{(8)}]g\rangle + O(v^2)|Q\bar{Q}[^3P_J^{(1,8)}]gg\rangle + \cdots, \tag{2}$$

where the superscript 1 or 8 labels the color configuration of the Fock components.

Following the NRQCD factorization formalism, the scattering amplitude of the process $e^-(p_1)+e^+(p_2)\to\gamma^*\to c\bar{c}(^{2S+1}L_J^{(1,8a)})(p)+c(p_c)+\bar{c}(p_{\bar{c}})$ in Figs. 1 and 2 is given by

$$\begin{aligned}\mathcal{A}(e^-(p_1)+e^+(p_2)\to c\bar{c}(^{2S+1}L_J^{(1,8a)})(p)+c(p_c)+\bar{c}(p_{\bar{c}})) &= \sqrt{C_L}\sum_{L_zS_z}\sum_{s_1s_2}\sum_{jk}\langle s_1;s_2|SS_z\rangle\langle LL_z;SS_z|JJ_z\rangle\langle 3j;\bar{3}k|1,8a\rangle \\ &\times\begin{cases}\mathcal{A}(e^-(p_1)+e^+(p_2)\to c_j(p/2;s_1)+\bar{c}_k(p/2;s_2)+c_l(p_c/2;s_3)+\bar{c}_i(p_{\bar{c}}/2;s_4)) & (L=S),\\ \epsilon_\alpha^*(L_Z)\mathcal{A}^\alpha(e^-(p_1)+e^+(p_2)\to c_j(p/2;s_1)+\bar{c}_k(p/2;s_2)+c_l(p_c/2;s_3)+\bar{c}_i(p_{\bar{c}}/2;s_4)) & (L=P),\end{cases}\end{aligned} \tag{3}$$

where $c\bar{c}(^{2S+1}L_J^{(1,8a)})$ is the intermediate $c\bar{c}$ pair produced at short distance, which subsequently evolves into a specific charmonium state at long distance, and $\mathcal{A}^\alpha$ is the derivative of the amplitude with respect to the relative momentum between the quark and antiquark in the bound state. For the case of the color-singlet state, the coefficient C_L can be related to the origin of the radial wave function (or its derivative) of the bound state as

$$C_S=\frac{1}{4\pi}|R_S(0)|^2, \quad C_P=\frac{3}{4\pi}|R_P'(0)|^2. \tag{4}$$

The spin projection operator can be defined as [19]

$$P_{SS_z}(p;q)\equiv\sum_{s_1s_2}\langle s_1;s_2|SS_z\rangle v\left(\frac{p}{2}+q;s_1\right)\bar{u}\left(\frac{p}{2}-q;s_2\right). \tag{5}$$

We list the spin projection operators and their derivatives with respect to the relative momentum, which we will use in the calculations, as

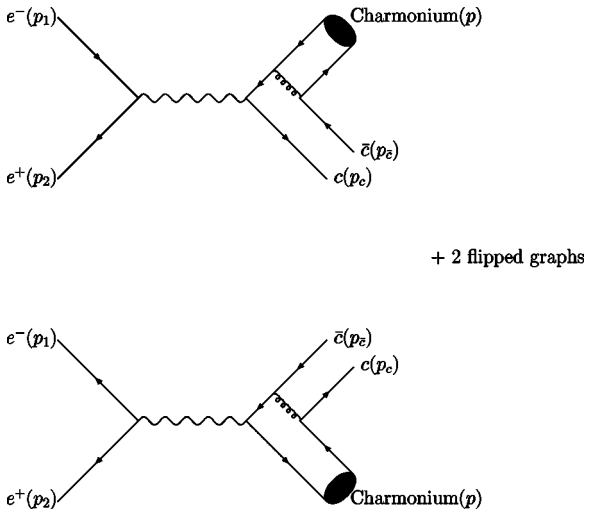

FIG. 1. Feynman diagrams for $e^+ + e^- \to \gamma^* \to$ charmonium $+ c\bar{c}$.

$$P_{00}(p,0) = \frac{1}{2\sqrt{2}} \gamma_5 (\not{p} + 2m_c), \tag{6}$$

$$P_{1S_Z}(p,0) = \frac{1}{2\sqrt{2}} \not{\epsilon}(S_z)(\not{p} + 2m_c), \tag{7}$$

$$P^{\alpha}_{1S_z}(p,0) = \frac{1}{4\sqrt{2}m_c}[\gamma^{\alpha} \not{\epsilon}^*(S_z)(\not{p} + 2m_c) - (\not{p} - 2m_c)\not{\epsilon}(S_z)\gamma^{\alpha}]. \tag{8}$$

For P-wave states we need further relations to reduce the polarizations:

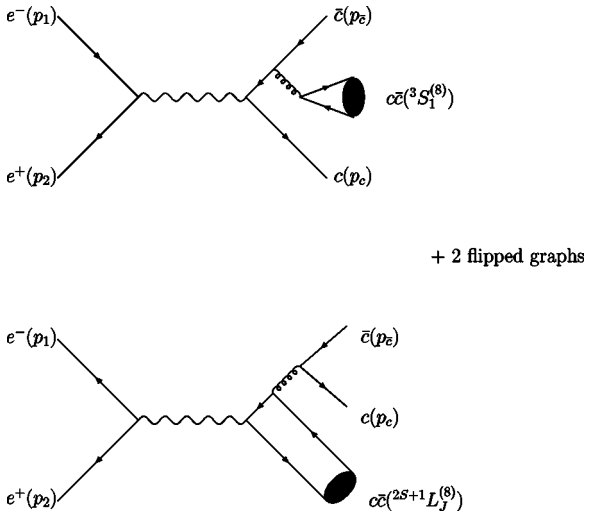

FIG. 2. Feynman diagrams for $e^+ + e^- \to \gamma^* \to c\bar{c}(^{2S+1}L_J^{(8)}) + c\bar{c}$.

$$\sum_{L_Z S_Z} \epsilon^{*\alpha}(L_Z)\epsilon^{*\beta}(S_Z)\langle 1L_Z; 1S_Z | J=0 J_Z=0\rangle = \frac{1}{\sqrt{3}}\left(-g^{\alpha\beta} + \frac{p^{\alpha}p^{\beta}}{M^2}\right),$$

$$\sum_{L_Z S_Z} \epsilon^{*\alpha}(L_Z)\epsilon^{*\beta}(S_Z)\langle 1L_Z; 1S_Z | J=1 J_Z\rangle = -\frac{i}{\sqrt{2}M}\epsilon^{\alpha\beta\lambda\kappa} p_{\kappa} \epsilon^*_{\lambda}(J_z),$$

$$\sum_{L_Z S_Z} \epsilon^{*\alpha}(L_Z)\epsilon^{*\beta}(S_Z)\langle 1L_Z; 1S_Z | J=1 J_Z\rangle = \epsilon^{*\alpha\beta}(J_Z), \tag{9}$$

where M is the mass of the charmonium, which equals $2m_c$ in the nonrelativistic approximation.

The calculation of cross sections for $e^- + e^+ \to \gamma^* \to$ charmonium $+ c\bar{c}$ is straightforward. Using the definition in Ref. [6] we get the differential cross section as follows:

$$\frac{d\sigma(e^+ + e^- \to \gamma^* \to \text{charmonium} + c\bar{c})}{dz} = \frac{4C_L \alpha^2 \alpha_s^2}{81 m_c}\left(S(z) + \frac{\alpha(z)}{3}\right), \tag{10}$$

where $L=S$ for S-wave, $L=P$ for P-wave, and $z = 2E_{J/\psi}/\sqrt{s}$. The functions $S(z)$ and $\alpha(z)$ for different charmonium states are given in the Appendix.

With Eq. (10) we can evaluate the inclusive cross sections for η_c, J/ψ, and χ_{cJ}. The input parameters used in the numerical calculations are [20]

$$m_e = 0, \quad m_c = 1.5 \text{ GeV}, \quad \alpha_s(2m_c) = 0.26, \quad \alpha = 1/137, \tag{11}$$

$$|R_S(0)|^2 = 0.81 \text{ GeV}^3, \quad |R_P(0)'|^2 = 0.075 \text{ GeV}^5. \tag{12}$$

Now we give the numerical results at the Belle and BaBar energy $\sqrt{s} = 10.6$ GeV:

$$\sigma(e^+ + e^- \to \gamma^* \to \eta_c + c\bar{c}) = 58.7 \text{ fb}, \tag{13}$$

$$\sigma(e^+ + e^- \to \gamma^* \to J/\psi + c\bar{c}) = 148 \text{ fb}, \tag{14}$$

$$\sigma(e^+ + e^- \to \gamma^* \to \chi_{c0} + c\bar{c}) = 48.8 \text{ fb}, \tag{15}$$

$$\sigma(e^+ + e^- \to \gamma^* \to \chi_{c1} + c\bar{c}) = 13.5 \text{ fb}, \tag{16}$$

$$\sigma(e^+ + e^- \to \gamma^* \to \chi_{c2} + c\bar{c}) = 6.30 \text{ fb}. \tag{17}$$

The J/ψ production rate is in agreement with other references [6,8,9] after taking into account the differences in the values of the input parameters. In the $z \gg \delta$ limit, where δ is

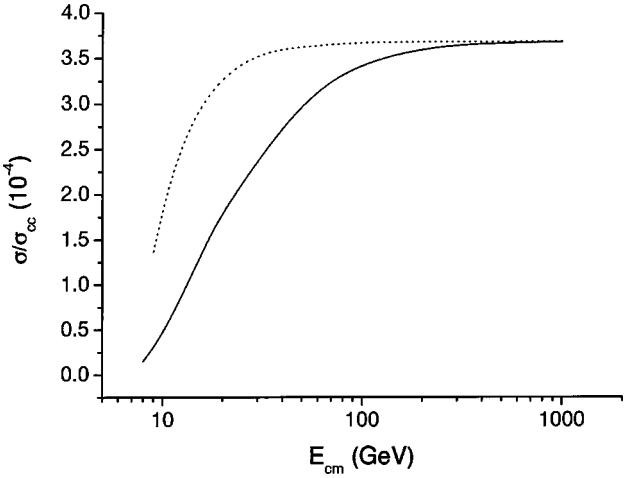

FIG. 3. Cross sections for $e^+e^-\to\eta_c+c\bar{c}$ plotted against the center-of-mass energy. The dotted line illustrates the fragmentation calculation and the solid line illustrates the complete calculation. The cross sections are in units of $\sigma_{cc}=\sigma(e^++e^-\to\gamma^*\to c\bar{c})$ times 10^{-4}.

defined as $4m_c/\sqrt{s}$, the approximate fragmentation results will be equivalent to the complete calculations. This is another check for the validity of the complete calculation. Here the fragmentation cross sections are written as

$$\sigma_{frag}(e^++e^-\to\gamma^*\to\text{charmonium}+c\bar{c}) = 2\sigma(e^++e^-\to c\bar{c})\int_\delta^1 \mathcal{D}_{c\to\text{charmonium}}(z)dz, \tag{18}$$

where $\mathcal{D}(z)$ are the charm quark fragmentation functions into S-wave [21] or P-wave [22] charmonia.

The cross sections obtained in the complete calculation and in the fragmentation approximation as functions of the center-of-mass energies are plotted in Figs. 3–7. All these cross sections are in units of $\sigma_{cc}=\sigma(e^++e^-\to\gamma^*\to c\bar{c})$,

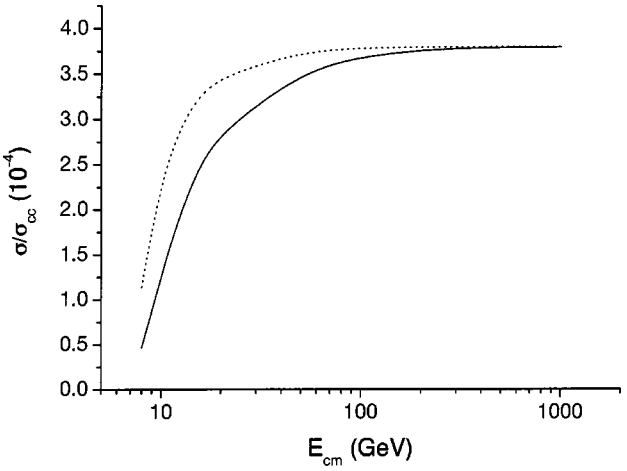

FIG. 4. Cross sections for $e^+e^-\to J/\psi+c\bar{c}$ plotted against the center-of-mass energy. The dotted line illustrates the fragmentation calculation and the solid line illustrates the complete calculation.

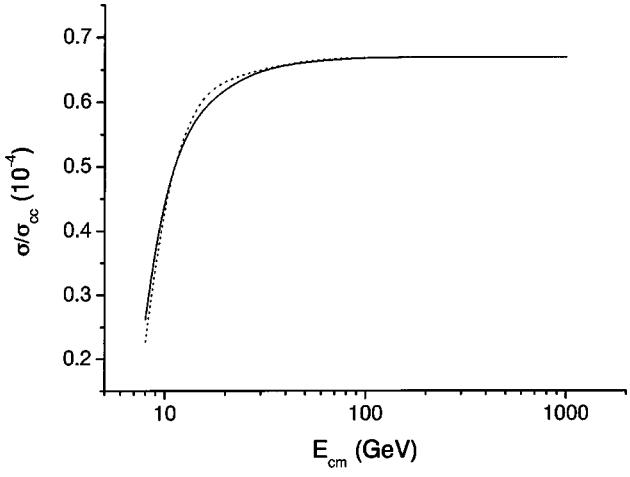

FIG. 5. Cross sections for $e^+e^-\to\chi_{c0}+c\bar{c}$ plotted against the center-of-mass energy. The dotted line illustrates the fragmentation calculation and the solid line illustrates the complete calculation.

the cross section for e^+e^- annihilating into the $c\bar{c}$ quark pair, times 10^{-4}. One can find that the cross sections in complete calculations and fragmentation approximations (all in units of the cross section for e^+e^- annihilating to the $c\bar{c}$ pair) are proportional to the fragmentation probabilities for the charm quark fragmentating into charmonia when the $\delta\ll 1$ limit is valid. This is just what the fragmentation approach describes. The results in these figures show that except for χ_{c0}, the differences between fragmentation results and complete calculations are large at low energies. At the Belle and BaBar energy $\sqrt{s}=10.6$ GeV, the ratios of complete calculations to fragmentation calculations are

$$\frac{\sigma(e^++e^-\to\gamma^*\to\text{charmonium}+c\bar{c})}{\sigma_{frag}(e^++e^-\to\gamma^*\to\text{charmonium}+c\bar{c})} = 0.28,\ 0.58,\ 0.25,\ \text{and}\ 0.25 \tag{19}$$

for η_c, J/ψ, χ_{c1}, and χ_{c2}, respectively. As the center-of-mass energy increases, the ratios of complete calculations to

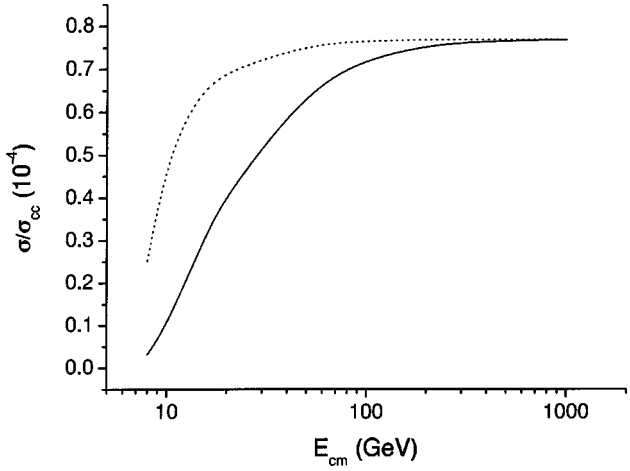

FIG. 6. Cross sections for $e^+e^-\to\chi_{c1}+c\bar{c}$ plotted against the center-of-mass energy. The dotted line illustrates the fragmentation calculation and the solid line illustrates the complete calculation.

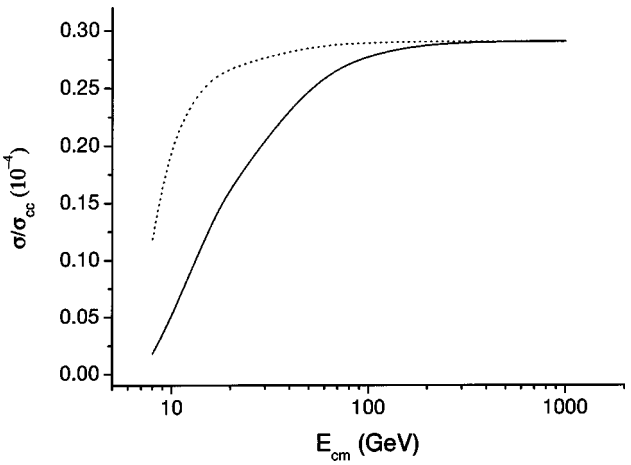

FIG. 7. Cross sections for $e^+e^-\to\chi_{c2}+c\bar{c}$ plotted against the center-of-mass energy. The dotted line illustrates the fragmentation calculation and the solid line illustrates the complete calculation.

fragmentation results increase and can reach 90% when the center-of-mass energy is over 100 GeV. Moreover, the cross sections are rather sensitive to the input parameters. If we choose $\alpha=1/134$, $\alpha_s=0.28$, and $m_c=1.48$ GeV at $\sqrt{s}=10.6$ GeV, the cross sections for η_c, J/ψ, and χ_{cJ} $(J=0,1,2)$ become 77.0, 192, 64.2, 18.3, and 8.48 fb, respectively.

III. COLOR-OCTET CONTRIBUTION TO J/ψ AND χ_{cJ} PRODUCTION VIA DOUBLE $c\bar{c}$ IN e^+e^- ANNIHILATION

We next estimate the color-octet contribution to J/ψ and χ_{cJ} production via double $c\bar{c}$ in e^+e^- annihilation. The Feynman diagrams are shown in Figs. 1 and 2.

In Fig. 1, the charmonium comes from the color-octet mediate states $c\bar{c}(^{2S+1}L_J^{(8)})$ by emitting soft gluons at long distances. Here the color-octet contribution can be obtained from the corresponding color-singlet contribution divided by a factor of $32\langle\mathcal{O}_1^H(^{2S+1}L_J)\rangle/3\langle\mathcal{O}_8^H(^{2S+1}L_J)\rangle$. The matrix elements $\langle\mathcal{O}_n^H(^{2S+1}L_J)\rangle$ can be extracted from the Tevatron data for J/ψ and χ_{cJ} production (see Ref. [23] for detailed discussions). Accordingly, with some unavoidable uncertainties in the present stage we assume them to be

$$\langle\mathcal{O}_1^{\psi}(^3S_1)\rangle=1.16\ \text{GeV}^3, \tag{20}$$

$$\langle\mathcal{O}_1^{\chi_{c1}}(^3P_1)\rangle=0.32\ \text{GeV}^5, \tag{21}$$

$$\langle\mathcal{O}_8^{\psi}(^3S_1)\rangle=1.06\times10^{-2}\ \text{GeV}^3, \tag{22}$$

$$\langle\mathcal{O}_8^{\psi}(^1S_0)\rangle/3\approx\langle\mathcal{O}_8^{\psi}(^3P_0)\rangle/m_c^2 \approx1.1\times10^{-2}\ \text{GeV}^3, \tag{23}$$

$$\langle\mathcal{O}_8^H(^3P_J)\rangle=(2J+1)\langle\mathcal{O}_8^H(^3P_0)\rangle, \tag{24}$$

$$\langle\mathcal{O}_8^{\chi_{c1}}(^3S_1)\rangle=1.0\times10^{-2}\ \text{GeV}^3. \tag{25}$$

With these values of the matrix elements, the color-octet contributions to J/ψ and χ_{cJ} in Fig. 1 are about two orders of magnitude smaller than the color-singlet contributions and, therefore, are negligible. For instance, the color-octet contributions from $^3S_1^{(8)}$, $^1S_0^{(8)}$, and $^3P_J^{(8)}$ $(J=0,1,2)$ to the $J/\psi c\bar{c}$ cross section are 0.12, 0.47, 1.1, 0.29, and 0.14 fb, respectively. In Fig. 2 the color-octet contributions come from four different (the upper two and the lower two) diagrams. With the $^3S_1^{(8)}$ contribution from the upper two diagrams in Fig. 2, the differential cross section reads

$$\frac{d\sigma_{octet}}{dz}=\frac{16\alpha^2\alpha_s^2\langle\mathcal{O}_8^H(^3S_1)\rangle}{27m_c}|\bar{M}|^2, \tag{26}$$

where $|\bar{M}|^2$ takes the form

$$|\bar{M}|^2=\frac{\pi}{12\delta^2s^2z(z-2)^2}\left\{-4z\sqrt{\frac{(1-z)(z^2-\delta^2)}{4+\delta^2-4z}}\times\{3\delta^4-12\delta^2(z-2)+16[10+z(z-10)]\}+(z-2)^2\{3\delta^4-8\delta^2(3z-4)+32[2+z(z-2)]\}\times\ln\left[\frac{z\sqrt{4+\delta^2-4z}+2\sqrt{(1-z)(z^2-\delta^2)}}{z\sqrt{4+\delta^2-4z}-2\sqrt{(1-z)(z^2-\delta^2)}}\right]\right\}. \tag{27}$$

The numerical results can be obtained by using the parameters given above and are

$$\sigma_{octet}(e^+e^-\to J/\psi c\bar{c})=4.5\ \text{fb}, \tag{28}$$

$$\sigma_{octet}(e^+e^-\to\chi_{c1}c\bar{c})=4.3\ \text{fb}. \tag{29}$$

The $^1S_0^{(8)}$ and $^3P_J^{(8)}$ $(J=0,1,2)$ color-octet contributions to $J/\psi c\bar{c}$ coming from the lower diagrams in Fig. 2 are 0.70, 0.18, 2.7, and 0.87 fb, respectively. Altogether with Figs. 1 and 2 the total color-octet contribution to $J/\psi c\bar{c}$ is only 7% of the color-singlet cross section. Since the color-octet contributions to $\chi_{cJ}c\bar{c}$ other than $^3S_1^{(8)}$ are of higher order of v, they are suppressed according to the velocity scaling rules. For $\chi_{c1}c\bar{c}$, the color-octet $^3S_1$ contribution is significant, which is about 32% of the color-singlet cross section. With the approximation of heavy quark spin symmetry, the contributions of the color octet $^3S_1$ to χ_{cJ} (from the color-octet $^3S_1$ mediate state to the color-singlet ^3P_J final state by an $E1$ transition) satisfy the ratio 1:3:5 for $J=0,1,2$, respectively. Their values are given by

$$\sigma_{octet}(e^+e^-\to\chi_{c0}c\bar{c})=1.4\ \text{fb}, \tag{30}$$

$$\sigma_{octet}(e^+e^-\to\chi_{c2}c\bar{c})=7.2\ \text{fb}. \tag{31}$$

We show the angular distribution and energy distribution for χ_{c1} in Figs. 8 and 9. One can see that the color-octet

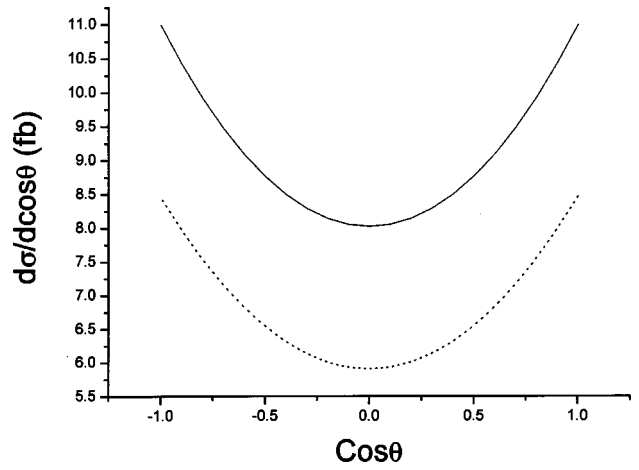

FIG. 8. Differential cross sections of the color-singlet (dotted line) and the sum of color-singlet and color-octet (solid line) contributions as functions of the production angle of χ_{c1}.

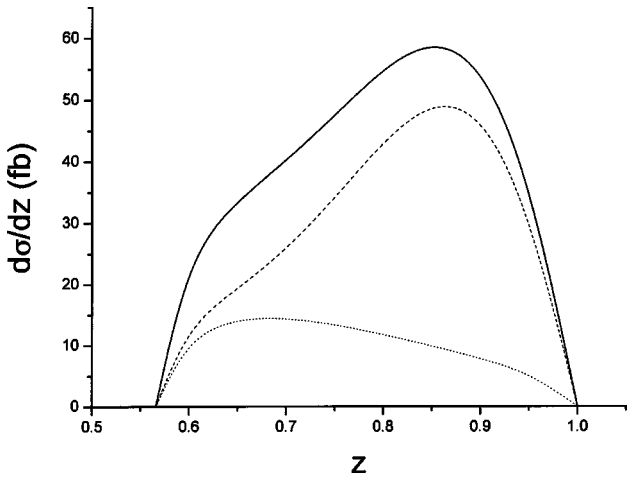

FIG. 9. Contributions to $d\sigma(e^+e^-\to\chi_{c1}c\bar{c})/dz$ from color-singlet (dashed line), color-octet (dotted line), and the sum of color-singlet and color-octet (solid line) contributions plotted against z.

contribution enhances the differential cross section significantly in the low-energy (small z) region.

IV. CONCLUSION

In summary, we have calculated the complete $O(\alpha_s^2)$ inclusive production cross sections for η_c, J/ψ, and χ_{cJ} $(J=0,1,2)$ plus $c\bar{c}$ in e^+e^- annihilation through a virtual photon. We considered both color-singlet and color-octet contributions, and give the analytical expressions for these cross sections. The complete color-singlet calculations are compared with the approximate fragmentation calculations as functions of the center-of-mass energy $\sqrt{s}$. We find that most of the fragmentation results substantially overestimate the cross sections (e.g., by a factor of ~ 4 for χ_{c1} and χ_{c2}) at the Belle and BaBar energy $\sqrt{s}=10.6$ GeV. The fragmentation results become a good approximation only when $\sqrt{s}$ is higher than about 100 GeV. We further calculated the color-octet contributions to these cross sections with analytical expressions. We find that while the color-octet contribution to J/ψ inclusive production via double charm is negligible (only about 7%), the color-octet contributions to χ_{c1} and χ_{c2} can be very significant. E.g., for the $\chi_{c1}c\bar{c}$ cross section, the ratio of the color-octet $^3S_1^{(8)}$ contribution to color-singlet contribution is about 32%. These results may serve as NRQCD predictions to compare with the experimental data observed or to be observed at Belle and BaBar.

ACKNOWLEDGMENTS

The authors thank Z.Z. Song for useful discussions. This work was supported in part by the National Natural Science Foundation of China, and the Education Ministry of China.

APPENDIX

In this appendix, we give the functions of S and α which are defined in Eq. (10):

$$
\begin{aligned}
S_{\eta_c} = \frac{4\pi}{3s^2\delta^2 z^3(z-2)^6(z^2-\delta^2)}\Bigg\{ & 4z\sqrt{\frac{(1-z)(z^2-\delta^2)}{4+\delta^2-4z}} \\
& \times[-96\delta^6(2+\delta^2)(4+\delta^2)+96\delta^6(64+22\delta^2+\delta^4)z-16\delta^2(1920-864\delta^2+532\delta^4+125\delta^6-2\delta^8)z^2 \\
& +8\delta^2(9984-5312\delta^2+488\delta^4+96\delta^6-\delta^8)z^3+2(6144-47872\delta^2+20800\delta^4-392\delta^6-110\delta^8+3\delta^{10})z^4 \\
& -4(6144-21376\delta^2+4256\delta^4+112\delta^6+9\delta^8)z^5+(14336-51328\delta^2+5472\delta^4+420\delta^6-3\delta^8)z^6 \\
& -4(1536-3168\delta^2+352\delta^4+\delta^6)z^7+8(864-36\delta^2+13\delta^4)z^8-32(112+11\delta^2)z^9+768z^{10}] \\
& -3\delta^2(z-2)^4[8\delta^6(2+\delta^2)-96\delta^6 z-2\delta^2(192-48\delta^2+8\delta^4-\delta^6)z^2+16\delta^2(8+6\delta^2-\delta^4)z^3 \\
& +\delta^2(192+40\delta^2-\delta^4)z^4+8(32-4\delta^2+\delta^4)z^5-8(48+\delta^2)z^6]\ln\frac{z\sqrt{4+\delta^2-4z}+2\sqrt{(1-z)(z^2-\delta^2)}}{z\sqrt{4+\delta^2-4z}-2\sqrt{(1-z)(z^2-\delta^2)}}\Bigg\},
\end{aligned}
\tag{A1}
$$

$$\alpha_{\eta_c}=\frac{4\pi}{3s^2\delta^2z^3(z-2)^6(z^2-\delta^2)}\left\{4z\sqrt{\frac{(1-z)(z^2-\delta^2)}{4+\delta^2-4z}}\right.$$
$$\times[96\delta^6(4+\delta^2)(6+\delta^2)-96\delta^6(64+18\delta^2+\delta^4)z+16\delta^2(2688+608\delta^2+428\delta^4+43\delta^6-2\delta^8)z^2$$
$$-8\delta^2(17664+3264\delta^2+184\delta^4-96\delta^6-\delta^8)z^3+2(6144+89344\delta^2+7744\delta^4-2024\delta^6-174\delta^8-3\delta^{10})z^4$$
$$-4(6144+22656\delta^2-1376\delta^4-512\delta^6-35\delta^8)z^5+(14336+5504\delta^2-5152\delta^4-732\delta^6-3\delta^8)z^6$$
$$-4(1536-1760\delta^2-416\delta^4+\delta^6)z^7+8(864-196\delta^2+13\delta^4)z^8-32(112+11\delta^2)z^9+768z^{10}]$$
$$+3\delta^2(z-2)^4[8\delta^6(6+\delta^2)-32\delta^6z-2\delta^2(64+48\delta^2+16\delta^4-\delta^6)z^2+16\delta^2(12-\delta^2)(2+\delta^2)z^3$$
$$\left.-(1024+320\delta^2-88\delta^4-\delta^4)z^4+8(96-28\delta^2-\delta^4)z^5+8(16+\delta^2)z^6]\ln\frac{z\sqrt{4+\delta^2-4z}+2\sqrt{(1-z)(z^2-\delta^2)}}{z\sqrt{4+\delta^2-4z}-2\sqrt{(1-z)(z^2-\delta^2)}}\right\}, \quad \text{(A2)}$$

$$S_\psi=\frac{4\pi}{s^2\delta^2z^3(z-2)^6(z^2-\delta^2)}\left\{4z\sqrt{\frac{(1-z)(z^2-\delta^2)}{4+\delta^2-4z}}\right.$$
$$\times[-32\delta^4(4+\delta^2)(48+22\delta^2+3\delta^4)+32\delta^4(768+400\delta^2+66\delta^4+3\delta^6)z-16\delta^2(384+1920\delta^2+556\delta^4+29\delta^6-2\delta^8)z^2$$
$$+8\delta^2(1792+128\delta^2-568\delta^4-80\delta^6-\delta^8)z^3+2(2048-11008\delta^2+10752\delta^4+3176\delta^6+98\delta^8+3\delta^{10})z^4$$
$$-4(4096-7808\delta^2+3424\delta^4+600\delta^6+17\delta^8)z^5+(38912-20608\delta^2+4544\delta^4+508\delta^6-3\delta^8)z^6$$
$$-4(13312-800\delta^2+120\delta^4-3\delta^6)z^7+8(4512-20\delta^2-15\delta^4)z^8-32(336-\delta^2)z^9+1280z^{10}]$$
$$-\delta^2(z-2)^4[8\delta^4(48+22\delta^2+3\delta^4)-32\delta^4(24+5\delta^2)z-2\delta^2(448+16\delta^2+8\delta^4-3\delta^6)z^2$$
$$+16\delta^2(56-10\delta^2-5\delta^4)z^3+\delta^2(1152+272\delta^2-3\delta^4)z^4$$
$$\left.+8(32-92\delta^2+5\delta^4)z^5-56(16+\delta^2)z^6+512z^7]\ln\frac{z\sqrt{4+\delta^2-4z}+2\sqrt{(1-z)(z^2-\delta^2)}}{z\sqrt{4+\delta^2-4z}-2\sqrt{(1-z)(z^2-\delta^2)}}\right\}, \quad \text{(A3)}$$

$$\alpha_\psi=\frac{4\pi}{s^2\delta^2z^3(z-2)^6(z^2-\delta^2)}\left\{4z\sqrt{\frac{(1-z)(z^2-\delta^2)}{4+\delta^2-4z}}\right.$$
$$\times[32\delta^4(4+\delta^2)(16+2\delta^2+3\delta^4)-32\delta^4(256+48\delta^2+22\delta^4+3\delta^6)z+16\delta^2(1152+1024\delta^2-140\delta^4-53\delta^6-2\delta^8)z^2$$
$$-8\delta^2(5376+128\delta^2-1576\delta^4-240\delta^6-\delta^8)z^3+2(2048-768\delta^2-19968\delta^4-6968\delta^6-350\delta^8-3\delta^{10})z^4$$
$$-4(4096-20096\delta^2-11168\delta^4-1208\delta^6-43\delta^8)z^5+(38912-75392\delta^2-16960\delta^4-996\delta^6-3\delta^8)z^6$$
$$-4(13312-6304\delta^2-872\delta^4-3\delta^6)z^7+8(4512-500\delta^2-15\delta^4)z^8-32(336-\delta^2)+1280z^{10}]$$
$$+\delta^2(z-2)^4[8\delta^4(16+2\delta^2+3\delta^4)-32\delta^4(8-\delta^2)z-2\delta^2(320-272\delta^2+64\delta^4-3\delta^6)z^2+16\delta^2(40-54\delta^2-5\delta^4)z^3$$
$$\left.-(1024-720\delta^4-3\delta^6)z^4+8(96-36\delta^2-5\delta^4)z^5+8(80+7\delta^2)z^6-512z^7]\ln\frac{z\sqrt{4+\delta^2-4z}+2\sqrt{(1-z)(z^2-\delta^2)}}{z\sqrt{4+\delta^2-4z}-2\sqrt{(1-z)(z^2-\delta^2)}}\right\}, \quad \text{(A4)}$$

$$S_{\chi_{c0}}=\frac{8\pi}{9s^3\delta^4z^5(z-2)^8(z^2-\delta^2)}\left\{-4z\sqrt{(1-z)(z^2-\delta^2)(4+\delta^2-4z)}\right.$$
$$\times[2304\delta^{10}-1152\delta^8(26+5\delta^2)z+192\delta^6(640+464\delta^2+35\delta^4)z^2+96\delta^4(1152-4816\delta^2-1136\delta^4-43\delta^6)z^3$$
$$+16\delta^2(4608-33024\delta^2+44752\delta^4+4360\delta^6+75\delta^8)z^4-8\delta^2(21504-123392\delta^2+78448\delta^4+2884\delta^6-45\delta^8)z^5$$

$$
\begin{aligned}
&-4(12288-156672\delta^2+244224\delta^4-78128\delta^6-512\delta^8+21\delta^{10})z^6-2(24576+549888\delta^2-356096\delta^4\\
&+41744\delta^6+80\delta^8-9\delta^{10})z^7-8(4608-93952\delta^2+45728\delta^4-1206\delta^6+27\delta^8)z^8\\
&+(487424-208384\delta^2+119424\delta^4+696\delta^6-9\delta^8)z^9-4(155904+4160\delta^2+5216\delta^4-21\delta^6)z^{10}\\
&+16(22976+1480\delta^2+85\delta^4)z^{11}-480(232+11\delta^2)z^{12}+15104z^{13}]\\
&+3\delta^2(z-2)^4[-192\delta^{10}+96\delta^8(26+3\delta^2)z-64\delta^6(160+75\delta^2+3\delta^4)z^2-16\delta^4(576-1664\delta^2-183\delta^4-2\delta^6)z^3\\
&-4\delta^2(1536-4608\delta^2+4016\delta^4+152\delta^6+5\delta^8)z^4+2\delta^2(11264-23424\delta^2-160\delta^4+106\delta^6+3\delta^8)z^5\\
&+4(2048-4224\delta^2+9952\delta^4+248\delta^6-27\delta^8)z^6-(20480-22528\delta^2+5312\delta^4-368\delta^6+3\delta^8)z^7\\
&+4(4096-6496\delta^2-600\delta^4+17\delta^6)z^8-16(320-472\delta^2+7\delta^4)z^9\\
&+32(48+\delta^2)z^{10}]\ln\frac{z\sqrt{4+\delta^2-4z}+2\sqrt{(1-z)(z^2-\delta^2)}}{z\sqrt{4+\delta^2-4z}-2\sqrt{(1-z)(z^2-\delta^2)}}\Bigg\}, \qquad \text{(A5)}
\end{aligned}
$$

$$
\begin{aligned}
\alpha_{\chi_{c0}}=&\frac{8\pi}{9s^3\delta^4z^5(z-2)^8(z^2-\delta^2)}\Bigg\{4z\sqrt{(1-z)(z^2-\delta^2)(4+\delta^2-4z)}\\
&\times[2304\delta^{10}-5760\delta^8(6+\delta^2)z+192\delta^6(896+424\delta^2+35\delta^4)z^2+96\delta^4(384-4528\delta^2-904\delta^4-43\delta^6)z^3\\
&+16\delta^2(1536+3840\delta^2+23536\delta^4+2992\delta^6+75\delta^8)z^4-8\delta^2(52224+8704\delta^2+3280\delta^4+1924\delta^6-45\delta^8)z^5\\
&+4(12288+70656\delta^2-51200\delta^4-34224\delta^6-232\delta^8-21\delta^{10})z^6\\
&+2(24576+336896\delta^2+133888\delta^4+53904\delta^6+376\delta^8+9\delta^{10})z^7\\
&+16(2304-62720\delta^2-11280\delta^4-2191\delta^6-30\delta^8)z^8-(487424-605696\delta^2-61312\delta^4-7016\delta^6-9\delta^8)z^9\\
&+4(155904-40768\delta^2-2560\delta^4-21\delta^6)z^{10}-16(22976-504\delta^2+85\delta^4)z^{11}+480(232+11\delta^2)z^{12}-15104z^{13}]\\
&+3\delta^2(z-2)^4[192\delta^{10}-288\delta^8(10+\delta^2)z+64\delta^6(224+59\delta^2+3\delta^4)z^2+16\delta^4(192-1248\delta^2-121\delta^4-2\delta^6)z^3\\
&+4\delta^2(512-12288\delta^2+2384\delta^4-56\delta^6+5\delta^8)z^4+2\delta^2(3072+35968\delta^2-160\delta^4+50\delta^6-3\delta^8)z^5\\
&-4(2048-4992\delta^2+8224\delta^4-408\delta^6-23\delta^8)z^6+(12288-51200\delta^2-3008\delta^4-1456\delta^6-3\delta^8)z^7\\
&-4(2048-8992\delta^2-1224\delta^4-17\delta^6)z^8+16(192-616\delta^2-7\delta^4)z^9\\
&+32(16+\delta^2)z^{10}]\ln\frac{z\sqrt{4+\delta^2-4z}+2\sqrt{(1-z)(z^2-\delta^2)}}{z\sqrt{4+\delta^2-4z}-2\sqrt{(1-z)(z^2-\delta^2)}}\Bigg\}, \qquad \text{(A6)}
\end{aligned}
$$

$$
\begin{aligned}
S_{\chi_{c1}}=&\frac{-8\pi}{3s^3\delta^4z^5(z-2)^8(z^2-\delta^2)}\Bigg\{4z\sqrt{\frac{(1-z)(z^2-\delta^2)}{(4+\delta^2-4z)}}\\
&\times[2304\delta^8(3+\delta^2)(4+\delta^2)-1152\delta^6(192+208\delta^2+62\delta^4+5\delta^6)z\\
&+192\delta^4(3072+6400\delta^2+3568\delta^4+668\delta^6+35\delta^8)z^2-96\delta^4(26624+27808\delta^2+9992\delta^4+1276\delta^6+43\delta^8)z^3\\
&+16\delta^2(36864+277248\delta^2+195296\delta^4+50464\delta^6+4406\delta^8+75\delta^{10})z^4-8\delta^2(258048+521984\delta^2+302624\delta^4\\
&+57800\delta^6+2672\delta^8-45\delta^{10})z^5-4(98304-753664\delta^2-564992\delta^4-310048\delta^6-37736\delta^8-172\delta^{10}+21\delta^{12})z^6\\
&+2(983040-659456\delta^2+84480\delta^4-103008\delta^6-9000\delta^8-220\delta^{10}+9\delta^{12})z^7\\
&-(4784128+2330624\delta^2+1528576\delta^4+120800\delta^6+396\delta^8+117\delta^{10})z^8\\
&+(6914048+3928064\delta^2+1137792\delta^4+74544\delta^6+1900\delta^8-9\delta^{10})z^9\\
&-2(3100672+1294336\delta^2+200672\delta^4+8036\delta^6-9\delta^8)z^{10}+8(443392+116992\delta^2+8048\delta^4+35\delta^6)z^{11}
\end{aligned}
$$

$$
\begin{aligned}
&-64(20288+2808\delta^2+51\delta^4)z^{12}+512(544+33\delta^2)z^{13}-28672z^{14}]\\
&-3\delta^2(z-2)^4[-192\delta^8(3+\delta^2)+96\delta^6(48+28\delta^2+3\delta^4)z-16\delta^4(768+808\delta^2+217\delta^4+12\delta^6)z^2\\
&+16\delta^4(1600+652\delta^2+105\delta^4+2\delta^6)z^3+4\delta^2(7168-4352\delta^2-360\delta^4-59\delta^6-5\delta^8)z^4\\
&-2\delta^2(24576-3968\delta^2+1024\delta^4-64\delta^6-3\delta^8)z^5+\delta^2(17408-7296\delta^2+136\delta^4-51\delta^6)z^6\\
&-(8192-12800\delta^2-8576\delta^4-300\delta^6+3\delta^8)z^7+2(8192-6656\delta^2-1328\delta^4+17\delta^6)z^8\\
&-128(80-10\delta^2+\delta^4)z^9+128(24+5\delta^2)z^{10}]\ln\frac{z\sqrt{4+\delta^2-4z}+2\sqrt{(1-z)(z^2-\delta^2)}}{z\sqrt{4+\delta^2-4z}-2\sqrt{(1-z)(z^2-\delta^2)}}\Bigg\},
\end{aligned}
\tag{A7}
$$

$$
\begin{aligned}
\alpha_{\chi_{c1}}=&\frac{-8\pi}{3s^3\delta^4z^5(z-2)^8(z^2-\delta^2)}\Bigg\{-4z\sqrt{\frac{(1-z)(z^2-\delta^2)}{(4+\delta^2-4z)}}\\
&\times[2304\delta^8(1+\delta^2)(4+\delta^2)-1152\delta^6(64+80\delta^2+42\delta^4+5\delta^6)z+192\delta^4(1024+2432\delta^2\\
&+1360\delta^4+404\delta^6+35\delta^8)z^2-96\delta^4(8192+11872\delta^2+3640\delta^4+652\delta^6+43\delta^8)z^3\\
&+16\delta^2(110592+58624\delta^2+71328\delta^4+12864\delta^6+1522\delta^8+75\delta^{10})z^4\\
&-8\delta^2(724992-245504\delta^2-21024\delta^4-72\delta^6+136\delta^8-45\delta^{10})z^5\\
&+4(98304+1392640\delta^2-1900288\delta^4-349344\delta^6-20648\delta^8-1756\delta^{10}-21\delta^{12})z^6\\
&-2(983040-856064\delta^2-5078528\delta^4-704352\delta^6-37736\delta^8-724\delta^{10}-9\delta^{12})z^7\\
&+(4784128-7352320\delta^2-7412992\delta^4-760736\delta^6-20452\delta^8-447\delta^{10})z^8\\
&-(6914048-6197248\delta^2-3225472\delta^4-202576\delta^6-4772\delta^8-9\delta^{10})z^9\\
&+2(3100672-1243136\delta^2-376864\delta^4-15260\delta^6-9\delta^8)z^{10}-8(443392-47360\delta^2-10128\delta^4+35\delta^6)z^{11}\\
&+64(20288+472\delta^2+51\delta^4)z^{12}-512(544+33\delta^2)z^{13}+28672z^{14}]\\
&+3\delta^2(z-2)^4[-192\delta^8(1+\delta^2)+96\delta^6(16+12\delta^2+3\delta^4)z-16\delta^4(256+344\delta^2+59\delta^4+12\delta^6)z^2\\
&+16\delta^4(448+404\delta^2-9\delta^4+2\delta^6)z^3+4\delta^2(5120+1792\delta^2-856\delta^4+135\delta^6-5\delta^8)z^4\\
&-2\delta^2(16384+6016\delta^2-1088\delta^4+24\delta^6-3\delta^8)z^5+(32768-25600\delta^2-7040\delta^4-1864\delta^6-57\delta^8)z^6\\
&-(57344-81408\delta^2-11904\delta^4-884\delta^6-3\delta^8)z^7+2(16384-27648\delta^2-2384\delta^4-17\delta^6)z^8\\
&-128(48-118\delta^2-\delta^4)z^9-128(8+5\delta^2)z^{10}]\ln\frac{z\sqrt{4+\delta^2-4z}+2\sqrt{(1-z)(z^2-\delta^2)}}{z\sqrt{4+\delta^2-4z}-2\sqrt{(1-z)(z^2-\delta^2)}}\Bigg\},
\end{aligned}
\tag{A8}
$$

$$
\begin{aligned}
S_{\chi_{c2}}=&\frac{-8\pi}{9s^3\delta^4z^5(z-2)^8(z^2-\delta^2)}\Bigg\{4z\sqrt{\frac{(1-z)(z^2-\delta^2)}{(4+\delta^2-4z)}}\\
&\times[2304\delta^6(4+\delta^2)(144+57\delta^2+5\delta^4)-1152\delta^6(6336+3424\delta^2+558\delta^4+25\delta^6)z\\
&-192\delta^4(12288-82496\delta^2-39168\delta^4-5180\delta^6-175\delta^8)z^2+96\delta^4(125952-175584\delta^2-80408\delta^4-8852\delta^6-215\delta^8)z^3\\
&+16\delta^2(73728-1579776\delta^2+532640\delta^4+310240\delta^6+29834\delta^8+375\delta^{10})z^4\\
&-8\delta^2(651264-3396352\delta^2+224480\delta^4+323960\delta^6+24824\delta^8-225\delta^{10})z^5\\
&-4(98304-2469888\delta^2+3741440\delta^4-280928\delta^6-327288\delta^8-15148\delta^{10}+105\delta^{12})z^6\\
&+2(1179648-5492736\delta^2+1172992\delta^4-796064\delta^6-273016\delta^8-9940\delta^{10}+45\delta^{12})z^7\\
&-(7471104-8568832\delta^2-2286336\delta^4-864288\delta^6-131084\delta^8-1377\delta^{10})z^8
\end{aligned}
$$

$$+(14909440-4112384\delta^2-1213056\delta^4-33264\delta^6+1164\delta^8-45\delta^{10})z^9$$
$$-2(9654272+318976\delta^2+139168\delta^4+39524\delta^6+447\delta^8)z^{10}+8(1980416+242048\delta^2+25120\delta^4+883\delta^6)z^{11}$$
$$-64(119296+10832\delta^2+245\delta^4)z^{12}+1024(1840+73\delta^2)z^{13}-188416z^{14}]$$
$$-3\delta^2(z-2)^4[-192\delta^6(144+57\delta^2+5\delta^4)+96\delta^6(1008+304\delta^2+15\delta^4)z$$
$$+16\delta^4(4224-6392\delta^2-1731\delta^4-60\delta^6)z^2-16\delta^4(13632-916\delta^2-705\delta^4-10\delta^6)z^3$$
$$-4\delta^2(15360-56448\delta^2-8648\delta^4+433\delta^6+25\delta^8)z^4+2\delta^2(96256-29568\delta^2-13280\delta^4-340\delta^6+15\delta^8)z^5$$
$$+(16384-193536\delta^2-28672\delta^4+14680\delta^6+399\delta^8)z^6-5(8192-11776\delta^2-3712\delta^4+604\delta^6+3\delta^8)z^7$$
$$+2(10240+9728\delta^2-2784\delta^4-79\delta^6)z^8+512(4-47\delta^2+2\delta^4)z^9$$
$$+256(12+19\delta^2)z^{10}]\ln\frac{z\sqrt{4+\delta^2-4z}+2\sqrt{(1-z)(z^2-\delta^2)}}{z\sqrt{4+\delta^2-4z}-2\sqrt{(1-z)(z^2-\delta^2)}}\Bigg\}, \tag{A9}$$

$$\alpha_{\chi_{c2}}=\frac{8\pi}{9s^3\delta^4z^5(z-2)^8(z^2-\delta^2)}\Bigg\{4z\sqrt{\frac{(1-z)(z^2-\delta^2)}{(4+\delta^2-4z)}}$$
$$\times[2304\delta^6(4+\delta^2)(48+3\delta^2+5\delta^4)-1152\delta^6(2112+576\delta^2+170\delta^4+25\delta^6)z$$
$$-192\delta^4(6144-33088\delta^2-7296\delta^4-1428\delta^6-175\delta^8)z^2+96\delta^4(64512-102688\delta^2-16232\delta^4-1860\delta^6-215\delta^8)z^3$$
$$-16\delta^2(24576+1006848\delta^2-639968\delta^4-83584\delta^6-5006\delta^8-375\delta^{10})z^4$$
$$+8\delta^2(552960+3044608\delta^2-1287968\delta^4-209864\delta^6-6608\delta^8+225\delta^{10})z^5$$
$$+4(98304-4091904\delta^2-5157120\delta^4+2831904\delta^6+398216\delta^8+2884\delta^{10}-105\delta^{12})z^6$$
$$-2(1179648-15978496\delta^2-5100032\delta^4+4153696\delta^6+362376\delta^8+4228\delta^{10}-45\delta^{12})z^7$$
$$+(7471104-38830080\delta^2-5298944\delta^4+3212896\delta^6+207588\delta^8-285\delta^{10})z^8$$
$$-(14909440-29458432\delta^2-3163776\delta^4+769936\delta^6+15836\delta^8-45\delta^{10})z^9$$
$$+2(9654272-5982720\delta^2-388704\delta^4+34020\delta^6+447\delta^8)z^{10}-8(1980416-193664\delta^2-9312\delta^4+883\delta^6)z^{11}$$
$$+64(119296+3792\delta^2+245\delta^4)z^{12}-1024(1840+73\delta^2)z^{13}+188416z^{14}]$$
$$-3\delta^2(z-2)^4[-192\delta^6(48+3\delta^2+5\delta^4)+288\delta^6(112+8\delta^2+5\delta^4)z+16\delta^4(1920-3784\delta^2+71\delta^4-60\delta^6)z^2$$
$$-16\delta^4(6336-3660\delta^2+289\delta^4-10\delta^6)z^3-4\delta^2(13312-43392\delta^2+9928\delta^4-805\delta^6+25\delta^8)z^4$$
$$+2\delta^2(92160-76928\delta^2+6944\delta^4-676\delta^6+15\delta^8)z^5+(16384-322560\delta^2+121856\delta^4+10920\delta^6+365\delta^8)z^6$$
$$-(24576-248320\delta^2+96896\delta^4+5332\delta^6-15\delta^8)z^7+2(14336-40960\delta^2+12768\delta^4+79\delta^6)z^8$$
$$-512(36-55\delta^2+2\delta^4)z^9-256(4+19\delta^2)z^{10}]\ln\frac{z\sqrt{4+\delta^2-4z}+2\sqrt{(1-z)(z^2-\delta^2)}}{z\sqrt{4+\delta^2-4z}-2\sqrt{(1-z)(z^2-\delta^2)}}\Bigg\}. \tag{A10}$$

[1] CDF Collaboration, F. Abe *et al.*, Phys. Rev. Lett. **69**, 3704 (1992); **71**, 2537 (1993).

[2] G.T. Bodwin, L. Braaten, and G.P. Lepage, Phys. Rev. D **51**, 1125 (1995).

[3] M. Krämer, Nucl. Phys. B (Proc. Suppl.) **93**, 176 (2001).

[4] J.H. Kühn, J. Kaplan, and E.G.O. Safiani, Nucl. Phys. **B157**, 125 (1979); W.Y. Keung, Phys. Rev. D **23**, 2072 (1981); J.H. Kühn and H. Schneider, *ibid.* **24**, 2996 (1981); Z. Phys. C **11**, 263 (1981); L. Clavelli, Phys. Rev. D **26**, 1610 (1982).

[5] K. Hagiwara, A.D. Martin, and W.J. Stirling, Phys. Lett. B **267**, 527 (1991); V.M. Driesen, J.H. Kühn, and E. Mirkes, Phys. Rev. D **49**, 3197 (1994).

[6] P. Cho and K. Leibovich, Phys. Rev. D **54**, 6690 (1996).

[7] E. Braaten and Y.-Q. Chen, Phys. Rev. Lett. **76**, 730 (1996).

[8] F. Yuan, C.F. Qiao, and K.T. Chao, Phys. Rev. D **56**, 321 (1997); **56**, 1663 (1997).
[9] S. Baek, P. Ko, J. Lee, and H.S. Song, J. Korean Phys. Soc. **33**, 97 (1998).
[10] V.V. Kiselev *et al.*, Phys. Lett. B **332**, 411 (1994).
[11] BaBar Collaboration, B. Aubert *et al.*, Phys. Rev. Lett. **87**, 162002 (2001).
[12] Belle Collaboration, K. Abe *et al.*, Phys. Rev. Lett. **88**, 052001 (2002).
[13] Belle Collaboration, K. Abe *et al.*, Phys. Rev. Lett. **89**, 142001 (2002).
[14] E. Braaten and Jungil Lee, Phys. Rev. D **67**, 054007 (2003); K.Y. Liu, Z.G. He, and K.T. Chao, Phys. Lett. B **557**, 45 (2003); K. Hagiwara, E. Kou, and C.F. Qiao, *ibid.* **570**, 39 (2003).
[15] B.L. Ioffe and D.E. Kharzeev, Phys. Rev. D **69**, 014016 (2004).
[16] A.V. Berezhnoy and A.K. Likhoded, hep-ph/0303145.
[17] K.Y. Liu, Z.G. He, and K.T. Chao, Phys. Rev. D **68**, 031501 (2003).
[18] A.V. Luchinsky, hep-ph/0305253.
[19] Kühn, Kaplan, and Safiani [4]; B. Guberina, J.H. Kühn, R.D. Peccei, and R. Rückl, Nucl. Phys. **B174**, 317 (1980); P. Cho and A.K. Leibovich, Phys. Rev. D **53**, 150 (1996).
[20] E.J. Eichten and C. Quigg, Phys. Rev. D **52**, 1726 (1995).
[21] E. Braaten, K. Cheung, and T.C. Yuan, Phys. Rev. D **48**, 4230 (1993).
[22] T.C. Yuan, Phys. Rev. D **50**, 5664 (1994); J.P. Ma, *ibid.* **53**, 1185 (1996).
[23] P. Cho and A.K. Leibovich, Phys. Rev. D **53**, 6203 (1996); **53**, 150 (1996); M. Beneke and M. Krämer, *ibid.* **55**, 5269 (1997).